Iranian Journal of Fuzzy Systems

Volume 22, Number 1, (2025), pp. 93-110

Original paper

University of Sistan and Baluchestan

A fuzzy driver assistance system design with active disturbance rejection in autonomous vehicles with longitudinal movement

M. R. Mohammadi Damabi [1], M. Pourgholi [2] and M. Nouri Manzar [3]

[1,2,3] *Faculty of Electrical Engineering, Shahid Beheshti University, Tehran*

m_pourgholi@sbu.ac.ir

Abstract

In this paper, a practical adaptive cruise control system (ACC) with two controller levels is addressed. The upper-level control scheme consists of distance and speed controllers. This controller generates the desired acceleration profile that must be followed as closely as possible by the lower-level controller. A fuzzy adaptive output feedback controller with very high precision produces this desired acceleration. Furthermore, an adaptive observer estimates the states that can't be measured. The lower-level controller adjusts the throttle and brake actuators. Also, in the lower level, the active disturbance rejection controller (ADRC) eliminates all of the internal and external disturbances applied to the car. The ADRC parameters are tuned via the particle swarm genetic optimization algorithm. The closed-loop stability and semi-globally uniformly ultimately boundedness of all the signals is proved. Also, the asymptotic convergence of the ADRC controller estimation error to zero is insured. To show the effectiveness of the proposed method, the proposed algorithm is compared with a predictive controller, and the performance superiority of the proposed method is demonstrated.

Keywords: Adaptive cruise control system, throttle angle, pressure on the brake pedal, vehicle longitudinal control, fuzzy adaptive controller, active disturbance rejection system.

1 Introduction

Today's cars are equipped with various functions and driver assistance systems that increase the level of safety and reduce driver fatigue and traffic load. With the progress of science and the design of precise and different sensors, the studies were inclined towards the design of a driver assistance system under the name of adaptive cruise control (ACC). The ACC systems have been developed to improve performance in different conditions. The main aim of the ACC system is to maintain a relatively safe distance with the car that moves in the same lane ahead of the host car. If there is no car in front of the host, the speed of the host car is maintained at the desired speed determined by the driver [7]. The ACC system should also be able to respond as smoothly as possible when the vehicle in front leaves the intended lane or a new car enters the lane from another lane. Although the ACC systems with high capabilities are the ultimate goal, the reference [7] is the first step to enter the discussion of driver assistance systems and has many defects that must be fixed. Therefore, in the following years, systems were designed to automatically control a car as much as possible. For example, the ACC system only can control speed and relative position at speeds higher than 30-40 Km/h. Hence, the stop-and-go maneuver system should be provided along with the ACC system, so the automated car can be used in urban driving and traffic conditions. This system was able to stop the car completely [18]. An extension of the ACC system is the use of a system that links cars [9] and also uses the connection between the car and the road structure [1].

The designed systems were developed over time to solve many of their problems, including the influence of environmental conditions (road slope, road condition) [2, 19], disturbance consideration on the system [28], the robustness of

Corresponding Author: M. Pourgholi

Received: June 2024; Revised: October 2024; Accepted: January 2025.

https://doi.org/10.22111/ijfs.2025.48966.8628

the system against parameter changes [4, 28], increasing traffic efficiency [15], ensuring safety and comfort of passengers [30], economical fuel consumption [23], string stability [12]. In 2003, Barkat, Peng, and Lee [3] used special methods to characterize the ACC car, which was effective in traffic flow. The reference [13] proposed an adaptive control of vehicle traction force for intelligent highway systems. For longitudinal control, resistive control, adaptive fuzzy control, and adaptive sliding mode control (ASMC), the self-driving model was nonlinear and complex. The longitudinal control of a group of cars through the Wavelet neural network and a robust controller is investigated in [10]. Yang [6] proposes the vehicle longitudinal acceleration control (tracking) for stop-and-go (SG) by using model matching and sliding mode control strategy. In 2007, Wang [26] suggested a safe algorithm for accelerating and decelerating. In [16], a non-linear adaptive model reference controller for vehicle longitudinal dynamic control was designed. Dynamic uncertainty and external disturbance are considered in the proposed scheme. The power transmission system consists of the throttle valve and automatic gearbox and is controlled by an optimal control strategy [11]. The dynamic programming technique was used to obtain the optimal gear ratio and gas valve opening value (which leads to maximum fuel saving). The adaptive traction control algorithm for intelligent transportation systems is addressed in [21] by using sliding mode control and the second Lyapunov method. The model predictive stategy proposed in [23] to minimize fuel consumption and trackability. Also, a constarined predictive model-based control stategy is presented in [8] for an ACC system. The predictive controller solves a constrained quadratic optimization. One of the basic challenges in the ACC systems was the accuracy of acceleration tracking by the low-level controller. Also, The ACC system encounters wide uncertainties and no accurate model is available; therefore, a vehicle dynamic model with low complexity is presented in [29].

In this paper, a two-level control strategy is addressed for the ACC system. The upper-level control scheme consists of distance and speed controllers. The upper-level controller generates the desired acceleration profile that must be followed as closely as possible by the lower-level controller. A fuzzy adaptive output feedback controller with very high precision produces this desired acceleration. Furthermore, an adaptive observer estimates the states that can't be measured. The lower-level controller adjusts the throttle and brake actuators. Also, in the lower level, the active disturbance rejection controller (ADRC) eliminates all of the internal and external disturbances applied to the car. The ADRC parameters are tuned via the particle swarm genetic optimization algorithm. The closed-loop stability and semi-globally uniformly ultimately boundedness of all the signals is proved.

In section 2, we describe two vehicles following dynamic, throttle, and brake actuators model and some preliminaries. In section 3, the design of the fuzzy controller and active disturbance rejection controller, which are used in a hierarchical structure, will be discussed; also, the stability of the closed-loop system will be checked, while in section 4, simulation results are provided to demonstrate the effectiveness of the method. Finally, conclusions are given in section 5.

2 Problem formulation and preliminaries

The system modeling consists of two parts: 1. Longitudinal car following model which is used to model the problem of chasing two cars, 2. Modeling of external forces like rolling resistance, aerodynamic drag, longitudinal traction force, the gravitational force that acts on vehicle body, and also, throttle and brake actuators model. In addition, an anti-brake system and traction control system to reduce wheel slippage is modeled [10, 14]-[22].

2.1 A. Longitudinal car-following model

A hierarchical structure is used to design the ACC system, which consists of two levels of upper and lower controllers. This structure is shown in Fig. 1.

There are two main reasons to explain the highly nonlinear behavior of longitudinal vehicle motion. First, the engine output is not linear and the transmission ratio and air resistance are also variable. Secondly, there is a time delay when the commands are executed by the operators, including the accelerator and brake pedal. In this tracking model, there are two cars, one in the front and the other in the back. The rear car is known as the host car (including the adaptive cruise control system) and the front car is known as the target car.

The system dynamical behavior of the car following is described by a state space model as

$$\begin{cases} \dot{X}(t) = AX(t) + Bu(t) + Ed(t) \\ Y(t) = CX(t), \end{cases} \tag{1}$$

where the states are

$$X^T = \begin{bmatrix} x_1 & x_2 & x_3 \end{bmatrix} = \begin{bmatrix} x_p - x_{cc} & v_p - v_{cc} & v_{cc} \end{bmatrix}. \tag{2}$$

The control signal u is the host car acceleration. The symbols x_p, x_{cc}, v_{cc} , v_p, and $d\,(t)$ denote the target car position, the host car position, the host car speed, the target car speed, and disturbance input such as $d\,(t) = \sin(2\pi t)$ respectively. The parameters of (1) are

$$A = \begin{bmatrix} 0 & 1 & 0 \\ 0 & 0 & 0 \\ 0 & 0 & 1 \end{bmatrix}, \quad B = \begin{bmatrix} 0 \\ -1 \\ 1 \end{bmatrix}, \quad E = \begin{bmatrix} 0 \\ 0 \\ 1 \end{bmatrix}.$$

$$C = \begin{bmatrix} 1 & 0 & 0 \end{bmatrix}$$

2.2 Actuator modeling

2.2.1 Throttle actuator modeling

If the acceleration signal generated from the low-level controller is positive, then this signal means opening the throttle to a certain angle depending on the amount of torque requested from the engine. The desired engine torque can be calculated as follows:

$$T_{engine} = \frac{\left| mu + mgf\cos(\theta) + \frac{1}{2} C_D A \rho_A v^2 + mg\sin(\theta) \right|}{\tau(\frac{\omega_t}{\omega_e}) i_g i_m \eta}, \tag{3}$$

where m is the mass of the vehicle, τ is the speed–torque ratio coefficient, R is tire radius, ω_t is the turbine blade speed, ω_e is the engine speed, i_g is the transmission ratio, i_m is the axle main reduction ratio, F_b is the braking force, f is the driving resistance coefficient, wind resistance coefficient show with C_D, A is the cross-sectional area of the car, ρ_A is the air density, and T_{engine} is the engine torque. Now the throttle opening angle should be calculated according to the required torque and the engine rotational speed. For this purpose, a tabular function called manifold absolute pressure (MAP) is designed, which calculates the throttle opening angle from the required torque and the rotational speed. For the required engine torque, the throttle opening angle is calculated as follows.

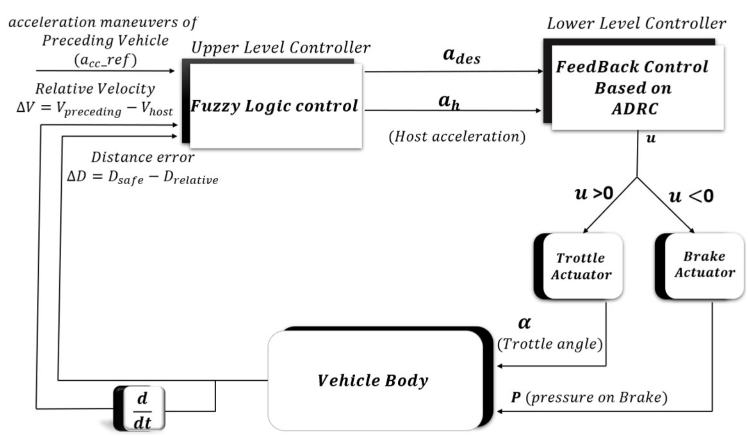

Figure 1: Schematic representation of the ACC system

$$\text{Estimated Throttle Angle}\,(\%) = \frac{\text{Torgue required at given accelerator position}}{\text{maxtorque at that speed}} * 100. \tag{4}$$

2.2.2 Brake actuator modeling

When the desired acceleration (the output signal from the lower-level controller is negative), the braking force can be calculated according to the following equation.

$$F_b = -mu - mgf\cos(\theta) - \frac{1}{2} C_D A \rho_A v^2 - mg\sin(\theta). \tag{5}$$

The desired pressure acting on the brake pedal is:

$$P_{des} = \frac{\left|-mu - mgf\cos(\theta) - \frac{1}{2}C_D A\rho_A v^2 - mg\sin(\theta)\right|}{k_b}, \tag{6}$$

where k_b is the linear proportional coefficient of the brake cylinder as follows:

$$K_b = \frac{T_{Fb} + T_{Rb}}{P_b R}, \tag{7}$$

where T_{Fb} is the proportional coefficient between the wheel and the brake cylinder pressure of the front axle, and T_{Rb} is the proportional coefficient between the wheel and the brake cylinder pressure of the rear axle.

In the next section, the proposed adaptive cruise control system is elaborated. The control architecture consists of higher-level and lower-level. The higher-level controller is a fuzzy adaptive controller with a performance criterion for the nonlinear system and the lower-level controller is an ADRC.

3 Adaptive cruise control architecture

The diagram in Fig.2 shows the core idea of the ACC system for designing the fuzzy adaptive controller. Consider a general system model as (8). where $x = [x_1, \ldots,\ x_n]^T$ is the state vector and u and y are system input and output, respectively. $d\,(t)$ denotes disturbance and $H(x,u)$ is an unknown Lipschitz function. It is assumed that only system output is measurable.

$$\begin{cases} \dot{x}_1(t) = x_2(t) \\ \quad \vdots \\ \dot{x}_{n-1}(t) = x_n(t) \\ \dot{x}_n(t) = H(x,u) + d(t) + bu(t) \\ y(t) = x_1(t). \end{cases} \tag{8}$$

The fuzzy adaptive controller objectives are: all the signals in the closed loop system remain bounded and the host car velocity v_h track reference signal $v_p(t)$ (velocity maneuvers of target vehicle) as closely as possible. The performance constraint imposed on tracking error $e\,(t) = v_p\,(t) - v_h(t)$ is as below [4, 17].

$$-\underline{\delta}\mu(t) < e(t) < \overline{\delta}\mu(t), \tag{9}$$

where $\underline{\delta}$ and $\overline{\delta}$ are some positive constants, with $\lim_{t\to\infty}\mu\,(t) = \mu_\infty > 0$ and $\mu\,(t)$ is a positive decreasing differentiable function which is considered as follows:

$$\mu(t) = (\mu_0 - \mu_\infty)e^{-kt} + \mu_\infty, \mu_0 > \mu_\infty > 0, k > 0. \tag{10}$$

Assumption 1 [7]: The reference signals $v_m(t)$ together with their derivatives up to order r $(r = 1, 2, \ldots, n)$ are smooth and bounded.

Assumption 2 [17]: For the unknown external disturbance $d\,(t)$, an unknown positive constant d^* exists such that $|d(t)| \leq d^*$.

3.1 A new fuzzy system

For a fuzzy system, the fuzzy propositions are defined in the form $IF - THEN$ and each of the fuzzy rules can be defined as follows

$$R^l{=}IF\ x_1\ is\ r_1^l\ and\ldots and\ x_n\ is\ r_n^l\ THEN\ z\ is\ G^l,$$

where F_i^l and G^l are fuzzy sets whose fuzzy membership functions are each identified by the names $\mu_{F_i^l}$, μ_{G^l}, and $l = 1, 2, \ldots, m$. With a singleton fuzzification strategy, product inference engine, and center average defuzzifier, the fuzzy system is

$$\hat{f}(x) = \frac{\sum_{l=1}^{m} z^l (\prod_{i=1}^{n} \mu_{F_i^l}(x_i))}{\sum_{l=1}^{m} (\prod_{i=1}^{n} \mu_{F_i^l}(x_i))}, \tag{11}$$

where $z^l = max_{z \in R} \mu_{G^l}$. The fuzzy basis is considered as

$$\xi^l(x) = \frac{\prod_{i=1}^{n} \mu_{F_i^l}(x_i)}{\sum_{l=1}^{m} (\prod_{i=1}^{n} \mu_{F_i^l}(x_i))}. \tag{12}$$

Therefore, the output is rewritten as

$$y(x) = W^T \xi(x) := \hat{f}(x|W), \tag{13}$$

where $W = [z^l\ ,\ \ldots, z^m]^T$, $\xi\,(x) = [\xi^1\,(x)\,, \ldots, \xi^m\,(x)]^T$.

$$W^T \xi(x) = W.\xi(x), \tag{14}$$

where the dot product of two vectors W *and* $\xi\,(x)$ is shown by $W.\xi\,(x)$.

$$W.\xi(x) = \|W\|\, \|\xi(x)\| \cos(\alpha), \tag{15}$$

that $0 \leq \alpha \leq \pi$ is the angle between two vectors W *and* $\xi\,(x)$. By defining $\|W\| \cos(\alpha) := \theta$, θ is the projection of the vector W on vector $\xi\,(x)$. Therefore, the fuzzy approximator has one tuning parameter θ as below:

$$\hat{f}(x|W) = W^T \xi(x) = \theta\, \|\xi(x)\|\,. \tag{16}$$

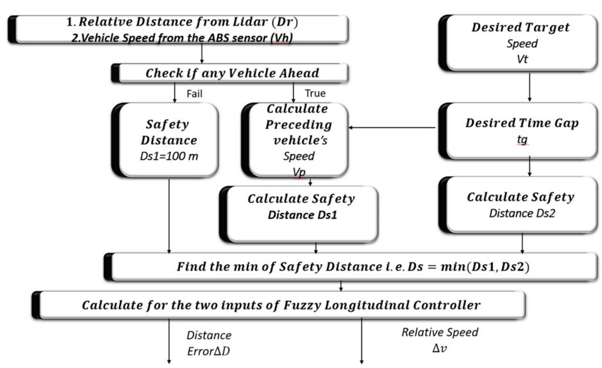

Figure 2: Architecture of the proposed fuzzy longitudinal controller

3.2 Upper-level controller: Adaptive fuzzy control

3.2.1 Defining transformed error

To satisfy the inequality (9), we consider a modified form of the error as

$$\varepsilon(t) = Arctanh((\frac{e(t)}{\mu(t)} - \frac{\overline{\delta} - \underline{\delta}}{2})/\frac{\overline{\delta} + \underline{\delta}}{2}), \tag{17}$$

where *Arctanh(.)* means the inverse hyperbolic tangent function. By using Eq. (17), the error is rewritten as

$$e(t) = \mu(t)(Tanh(\varepsilon(t))\frac{\overline{\delta}+\underline{\delta}}{2} + \frac{\overline{\delta}-\underline{\delta}}{2}), \tag{18}$$

and the following conditions are hold

$$\begin{cases} |Tanh(\varepsilon(t))| < 1, \forall \varepsilon(t) \in L_\infty \\ \lim\limits_{\varepsilon\to\infty} Tanh(\varepsilon(t)) = \pm 1 \end{cases} \tag{19}$$

Thus, we want to design a controller that guarantees the condition $\varepsilon(t) \in L_\infty$. This requires that

$$-\underline{\delta}\mu(t) < e(t) < \overline{\delta}\mu(t), \tag{20}$$

with the initial condition as

$$-\underline{\delta}\mu(0) < e(0) < \overline{\delta}\mu(0). \tag{21}$$

Therefore, in this paper, the control goal is to guarantee the condition $\varepsilon(t) \in L_\infty$ for the initial condition (21).

3.2.2 Adaptive fuzzy observer design

By defining $\overline{x} = \left[x^T, u^T\right]^T$ and using Lemma in [27] and (16), for every nonlinear unknown function such as $H(x,u)$, there exists a fuzzy system such as $\hat{H}(\overline{x}|\theta_H)$ such that

$$\hat{H}(\bar{x}|\theta_H) = W_H^T \xi_H(\bar{x}) = \theta_H \left\|\xi_H(\bar{x})\right\|. \tag{22}$$

That $\xi_H(\overline{x})$ is the fuzzy basis function vector, θ_H is the image of vector Y_H on the vector $\xi_H(\overline{x})$. The optimal parameter defines below:

$$\overset{*}{\theta}_H = \arg \min_{\theta_H\in\Omega_H} [\sup_{\bar{x}\in\bar{U}} |\theta_H \left\|\xi_H(\bar{x})\right\| - H(x,u)|], \tag{23}$$

where $\grave{\mathrm{U}}_H$ and $\overline{U}$ are bounded compact sets for θ_H and $\overline{x}$. Thus, for estimating the unmeasured states, a state observer is used. Suppose $\hat{x}$ is the estimated state vector and $\hat{\bar{x}} = [\hat{x}^T, u^T]^T$. The fuzzy adaptive observer is as follows:

$$\begin{cases} \dot{\hat{x}}(t) = A\hat{x}(t) + My(t) + P^{-1}C(\theta_H \left\|\xi_H(\hat{\bar{x}})\right\|) \\ \hat{y}(t) = C^T\hat{x}(t). \end{cases} \tag{24}$$

3.2.3 Error estimation transformation

The error is defined as

$$\hat{e}(t) = \hat{\upsilon}_p(t) - \hat{\upsilon}_h(t). \tag{25}$$

Also, the transformed error is

$$\hat{\varepsilon}(t) = Arctanh((\frac{\hat{e}(t)}{\mu(t)} - \frac{\overline{\delta}-\underline{\delta}}{2})/\frac{\overline{\delta}+\underline{\delta}}{2}). \tag{26}$$

The transformed error derivation is

$$\dot{\hat{\varepsilon}}(t) = \gamma(\dot{\hat{e}}(t) - \frac{\hat{e}(t)\dot{\mu}(t)}{\mu(t)}) = \gamma\dot{\hat{e}}(t) + \wp(\hat{e}(t), t). \tag{27}$$

Consider following transformed error estimation vector

$$\hat{E}(t) = [\hat{\varepsilon}(t), ..., \hat{\varepsilon}^{(r-1)}(t)]^T, \tag{28}$$

and the filtered transformed error estimations are defined as:

$$\hat{s}(t) = [\Lambda^T, 1]\hat{E}(t), \tag{29}$$

where $\Lambda = [\bar{\lambda}_1, ..., \bar{\lambda}_{r-1}]^T$is chosen properly in a form that the polynomial$s^{r-1} + \bar{\lambda}_{r-1}s^{r-2} + ... + \bar{\lambda}_1$ is Hurwitz. So, from it can be shown that [27]

$$\nu = [0, \Lambda^T]\hat{E}(t) + \gamma\hat{e}^{(r)}(t) + \wp(\hat{e}(t), t) + \gamma v_m^{(r)}(t). \tag{30}$$

3.2.4 Nassbaum function

A function $N(\xi)$ is known as a Nassbaum function if the following two conditions are hold [20, 27].

$$\lim_{s\to+\infty} \sup \frac{1}{2}\int_0^s N(\zeta)d\zeta = +\infty, \tag{31}$$

$$\lim_{s\to+\infty} \inf \frac{1}{2}\int_0^s N(\zeta)d\zeta = -\infty. \tag{32}$$

3.2.5 Adaptive fuzzy output feedback controller design

The controller designed in the section will be in the following form.

$$u(t) = R\hat{s}(t)u_0(t), \tag{33}$$

where $M_r = [\underbrace{0, ..., 0, -\hat{s}\gamma}_{r}]$ and $M = M_r * P^{-1} * C$. Also, we define

$$\Upsilon = \left\|R^{-1}v\right\| + \frac{1}{2}\left\|R^{-1}\hat{s}(t)\right\| + \|\theta_H(t)\| \, \|\xi_H(\hat{x})\| + 2\,\|R\hat{s}(t)\|\,. \tag{34}$$

The parameter matching rule for θ_H is as follows.

$$\dot{\theta}_H(t) = -\eta_H(\left\|\xi_H(\hat{\bar{x}})\right\|(\tilde{e}(t) + M) + l_H\theta_H(t)), \tag{35}$$

where $\tilde{e}(t) = \hat{e}(t) - e(t)$, $\eta_H > 0$. Also, $u_0(t)$ is designed as follows

$$u_0(t) = -\lambda_0 N(\zeta)\Upsilon^2. \tag{36}$$

And $\zeta(t)$is updated as

$$\dot{\zeta}(t) = \lambda_0\,\|R\hat{s}(t)\|^2\,\Upsilon^2, \tag{37}$$

where $N(\xi) = \exp(\xi^2)\cos(\frac{\pi}{2}\xi)$ and λ_0 is a positive constant.

3.3 Lower-level controller: Active disturbance rejection control

The active disturbance rejection control includes three parts, as shown in Fig. 3, the tracking differentiator, extended state observer, and nonlinear state error feedback. Since the vehicle experiences a certain delay in the process of executing the control signal, a first-order delay link is added before the ADRC feedback compensation control. The tracking differentiator is used to organize the desired transient dynamic process. Therefore, the output signal of the derivative part of the tracking differentiator should change gradually and the system's error should not be too large when the reference signal changes instantaneously. Contrary to the conventional method where N-order system states can be estimated with an N-order state observer, the extended state observer with *N+1* states is utilized. The added state in the extended state observer is used to estimate the total action required for model uncertainty and system disturbances compensation. The nonlinear state error feedback is the control law, which is the combination of the tracking differentiator signal and the action that comes from the extended state observer.

3.3.1 ADRC formulation

For the tracking differentiator part of ADRC, the following equations are defined. The following equations are the time optimal that guarantees the fastest convergence from a_1 to a_{des}.

$$\text{Tracking Differentator}\begin{cases} \dot{a}_1(t) = a_2(t) \\ \dot{a}_2(t) = fst(a_1(t) - a_{des}(t), a_1(t), \gamma, \omega) \end{cases}$$

where fst is

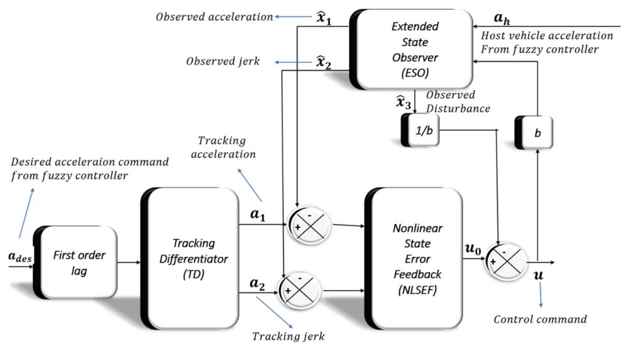

Figure 3: Principle of the lower-level control

$$\begin{cases} d = \gamma\omega^2 \\ \delta_0 = \omega^2 a_2(t) \\ y = a_1(t) + \delta_0 \\ \delta_1 = \sqrt{d(d + 8\,|y|)} \end{cases}$$

$$\begin{cases} \delta_2 = \delta_0 + sign(y)(a_1(t) - d)/2 \\ S_y = (sign(y + d) - sign(y - d))/2 \\ \delta = (\delta_0 + y - \delta_2)S_y + \delta_2 \\ S_\delta = (sign(\delta + d) - sign(\delta - d))/2 \\ fst = -\gamma(a_{des}/d - sign(a_{des}))S_\delta - \gamma sign(\delta) \end{cases} \tag{38}$$

Also, for extended state observer, we have the following extended state observer equations

$$\begin{cases} e(t) = \hat{x}_1(t) - a_h(t) \\ \dot{\hat{x}}_1(t) = \hat{x}_2(t) - \beta_1 e(t) \\ \dot{\hat{x}}_2(t) = \hat{x}_3(t) - \beta_2 fal(e(t), \alpha, \varepsilon) + bu(t) \\ \dot{\hat{x}}_3(t) = \beta_3 fal(e(t), \alpha, \varepsilon) \end{cases} \tag{39}$$

where fal is

$$fal(e(t), \alpha, \varepsilon) = \begin{cases} \frac{e(t)}{\varepsilon^{\alpha-1}}, |e| \le \varepsilon \\ |e(t)|^\alpha sign(e(t)), |e| > \varepsilon \end{cases}$$

Now the control signal u in the nonlinear state error feedback block is constructed as follows

$$\begin{cases} e_1(t) = a_1(t) - \hat{x}_1(t) \\ e_2(t) = a_2(t) - \hat{x}_2(t) \\ u_0(t) = k_1 fal(e_1(t), \alpha_1, \varepsilon) + k_2 fal(e_2(t), \alpha_2, \varepsilon) \\ u(t) = u_0(t) - \frac{\hat{x}_3(t)}{b} \end{cases} \tag{40}$$

where γ *and* ω are the filter factor and the speed factor respectively, k_1 *and* k_2 are weighting coefficients, ξ_1 , *and* ξ_2 are the error between the extended state observer and tracking differentiator, u_0 is the output of the nonlinear error feedback block, u is the output of the active disturbance rejection controller and z_3/b is the compensator of all internal and external disturbances. Table. 1 shows the effect of the

Table 1 Effectiveness of each parameter in Active Disturbance Rejection Control

	Parameters	Explanation
TD	γ	Direct relation with speed and convergence but amplify noise.
	ω	Direct relation with noise filtering but degradation of stability margin.
ESO	β_1	Inverse relation with overshoot, direct relation with rise time.
	β_2	Inverse relation with state space error and direct relation with amplifying fluctuation.
	β_3	Inverse relation with whole system disturbance estimation time and direct relation with fluctuation.
NLSEF	k_1	Direct relation with overshoot and fluctuation.
	k_2	Direct relation with fluctuations and inverse relation with speed of the system.

coefficients for the active disturbance rejection controller design. Note that the controller parameters do not depend on the precise model of the system and this feature makes the active disturbance rejection controller completely independent of the system model.

3.3.2 ADRC parameter tuning: Genetic particle swarm optimization algorithm

The efficiency of the active disturbance rejection controller is strongly dependent on its parameters. The active disturbance rejection controller designed in this section has 12 parameters and the effect of each parameter is given in Table 1. The use of a Genetic Particle Swarm Optimization (GPSO) algorithm for tuning ADRC parameters is an attractive approach that combines the exploration capabilities of genetic algorithms with the convergence properties of particle swarm optimization. GPSO typically offers a faster convergence speed compared to traditional optimization methods like grid search or simple genetic algorithms due to its hybrid nature, which uses the strengths of both genetic algorithms (exploration) and particle swarm optimization (exploitation). However, the convergence speed may vary based on the parameter settings (e.g., population size, mutation rate, etc.) and the complexity of the ADRC parameter space. Faster convergence can sometimes lead to suboptimal solutions if the algorithm does not sufficiently explore the parameter space. A balance must be established: while seeking a quick solution, one must ensure that the exploration is adequate to avoid local optima. This can be managed by adjusting parameters such as population diversity and mutation rates. The cost function is the integral of the error absolute value that the distance and speed difference of two cars from each other and is defined as follows:

$$J = \int_0^t (|e_1(t)| + |e_2(t)|)dt, \tag{41}$$

where $e_2(t) = \Delta V = V_{T\arg et} - V_{Host}$and $e_1(t) = D_{safe} - \Delta D,\ \Delta D = D_{T\arg et} - D_{Host}$.
The optimized parameters of the system are given in the Table. 2.

3.4 Close-loop system stability

A variable change is used and (8) is rewritten as

$$\begin{cases} \dot{x}_1(t) = x_2(t) \\ \vdots \\ \dot{x}_{n-1}(t) = x_n(t) \\ \dot{x}_n(t) = H(x,u) + d(t) + bu(t) \end{cases} \Rightarrow \begin{cases} \dot{x}_1(t) = x_2(t) \\ \vdots \\ \dot{x}_{n-1}(t) = x_n(t) \\ \dot{x}_n(t) = x_{n+1}(t) + bu(t) \\ \dot{x}_{n+1}(t) = h(x,u,d,\dot{d}) \end{cases} \tag{42}$$

$$h(x,u,d,\dot{d}) = \frac{d}{dt}(H(x,u) + d(t))$$

Assumption 3: Let the unknown function $h(x,u,d,\dot{d})$ be a global Lipschitz function for x.

Theorem 3.1. *If the system in (42) satisfies the assumptions (1)-(3), then the designed controller in (33) with adaptation lows (35) and (37) guarantees that all the signals are semi-globally uniformly ultimately bounded and also the performance criterion in (9) is satisfied. Moreover, the estimation error of the ADRC controller asymptotically converges to zero.*

Proof. Consider the following Lyapunov candidate function for the close loop system

$$V(t) = V_0(t) + \hat{s}^T(t)\hat{s}(t) + \frac{\Phi_H^2(t)}{2\eta_H} + Z(t). \tag{43}$$

That the terms used in this function are:

$$\begin{cases} V_0(t) = \frac{1}{2}\tilde{x}^T(t)P\tilde{x}(t) \\ \hat{s}(t) = [\Lambda^T, 1]\hat{E}(t) \Rightarrow \hat{E}(t) = [\hat{\varepsilon}(t), ..., \hat{\varepsilon}^{(r-1)}(t)]^T \\ \Phi_F(t) = \theta_F(t) - \theta_F{}^*(t), \eta_F > 0 \\ \Phi_f(t) = \theta_f(t) - \theta_f{}^*(t), \eta_f > 0 \\ Z(t) = \varsigma^T(t)P\varsigma(t) \end{cases} \tag{44}$$

where $\theta_f(t)$ is the estimation of $\theta_f{}^*(t)$and $\Phi_f(t) = \theta_f(t) - \theta_f{}^*(t)$. The similar definition could be used for $\Phi_F(t)$. Term $Z(t)$ is related to the lower-level controller estimation error that defines below. According to (42), $x(t) = [x_1(t), x_2(t), ..., x_{n+1}(t)]^T$ is the extended state variable vector. Assuming that b in (42) is known, the parameters estimation equations in ADRC define as follows.

$$\begin{aligned} &\dot{\hat{x}}_1(t) = \hat{x}_2(t) + \beta_1(x_1(t) - \hat{x}_1(t)), \\ &\quad\vdots \\ &\dot{\hat{x}}_{n-1}(t) = \hat{x}_n(t) + \beta_{n-1}(x_1(t) - \hat{x}_1(t)), \\ &\dot{\hat{x}}_n(t) = \hat{x}_{n+1}(t) + \beta_n(x_1(t) - \hat{x}_1(t)) + bu(t), \\ &\dot{\hat{x}}_{n+1}(t) = h(\hat{x}(t), u(t), w(t), \dot{w}(t)) + \beta_{n+1}(x_1(t) - \hat{x}_1(t)), \end{aligned} \tag{45}$$

where $\hat{x}(t) = [\hat{x}_1(t), \hat{x}_2(t), ..., \hat{x}_{n+1}(t)]^T$is the estimation state variable vector. The β_i parametrization for extended state observer in ADRC is

$$[\beta_1, \beta_2, ..., \beta_{n+1}] = [\omega_0\alpha_1, \omega_0{}^2\alpha_2, ..., \omega_0{}^{n+1}\alpha_{n+1}], \tag{46}$$

where $\omega_0 > 0$ and the parameters α_i is determined in a way that the characteristic polynomial $s^{n+1} + \alpha_1 s^n + ... + \alpha_n s + \alpha_{n+1}$ became Hurwitz. The parameter ω_0 is the observer bandwidth. By defining $\tilde{x}_i = x_i - \hat{x}_i, i = 1, 2, 3, ..., n+1$ and using (45), we define observer estimation error as follows:

$$\begin{aligned} &\dot{\tilde{x}}_1(t) = \tilde{x}_2(t) - \omega_0\alpha_1(\tilde{x}_1(t)), \\ &\quad\vdots \\ &\dot{\tilde{x}}_{n-1}(t) = \tilde{x}_n(t) - \omega_0{}^{n-1}\alpha_{n-1}(\tilde{x}_1(t)). \end{aligned}$$

$$\begin{aligned} &\dot{\tilde{x}}_1(t) = \tilde{x}_2(t) - \omega_0\alpha_1(\tilde{x}_1(t)), \\ &\quad\vdots \\ &\dot{\tilde{x}}_{n-1}(t) = \tilde{x}_n(t) - \omega_0{}^{n-1}\alpha_{n-1}(\tilde{x}_1(t)), \\ &\dot{\tilde{x}}_n(t) = \tilde{x}_{n+1}(t) - \omega_0{}^n\alpha_n(\tilde{x}_1(t)) + bu(t), \\ &\dot{\tilde{x}}_{n+1}(t) = h(x(t), u(t), w(t), \dot{w}(t)) -, \\ &h(\hat{x}(t), u(t), w(t), \dot{w}(t)) - \omega_0{}^{n+1}\alpha_{n+1}(\tilde{x}_1(t)). \end{aligned} \tag{47}$$

Assume, $\varsigma_i(t) = \frac{\tilde{x}_i(t)}{\omega_0{}^{i-1}}$ we have

$$\dot{\varsigma}(t) = \omega_0 A\varsigma(t) + B\frac{h(x(t), u(t), w(t), \dot{w}(t)) - h(\hat{x}(t), u(t), w(t), \dot{w}(t))}{\omega_0{}^n}, \tag{48}$$

where

$$A = \begin{bmatrix} -\alpha_1 & 1 & 0 & ... & 0 \\ -\alpha_2 & 0 & 1 & ... & 0 \\ \vdots\ \vdots & & \ddots & \vdots & \vdots \\ -\alpha_n & 0 & ... & 0 & 1 \\ -\alpha_{n+1} & 0 & ... & 0 & 0 \end{bmatrix}, B = \begin{bmatrix} 0 & 0 & ... & 0 & 1 \end{bmatrix}^T,$$

and α_i are selected in a way that matrix A is Hurwitz. In the following parts, the genetic particle swarm optimization algorithm is used to determine the parameters β_i. Since matrix A is Hurwitz, there exists a symmetric positive definite matrix P such that$A^T P + PA = -Q$, therefore, we define function

Table 2 Tuned ADRC parameters

TD	***ESO***	***NLEF***
$\boldsymbol{\gamma = 6}$ $\boldsymbol{\omega = 5}$	$\alpha = 2$, $\varepsilon = 0.1$ $b = 10^9$, $\beta_1 = 1$ $\beta_2 = 1$, $\beta_3 = 1$	$\alpha_1 = 2$, $\alpha_2 = 2$ $k_1 = 2$, $k_2 = 5$

$Z(t) = \varsigma^T(t)P\varsigma(t)$, so the time derivative of the Lyapunov candidate function in (43) is as follows.

$$\dot{V}(t) = \dot{V}_0(t) + \hat{s}^T(t)\dot{\hat{s}}(t) + \frac{\Phi_H(t)\dot{\theta}_H(t)}{\eta_H} + \dot{Z}(t). \tag{49}$$

Also, the derivation of term $Z(t)$ is

$$\dot{Z}(t) = \frac{\partial Z(t)}{\partial \varsigma(t)}\dot{\varsigma}(t), \tag{50}$$

where

$$\frac{\partial Z(t)}{\partial \varsigma(t)} = \frac{\partial(\varsigma^T(t)P\varsigma(t))}{\partial \varsigma(t)} = 2\varsigma^T(t)P.$$

Substituting (48) in (50), yields:

$$\begin{aligned}
&\dot{Z}(t) = 2\varsigma^T(t)P\dot{\varsigma}(t) = 2\varsigma^T(t)P[\omega_0 A\varsigma(t) + B\frac{h(x(t),u(t),d(t),\dot{d}(t)) - h(\hat{x}(t),u(t),d(t),\dot{d}(t))}{{\omega_0}^n}] = \\
&\omega_0\varsigma^T(t)PA\varsigma(t) + \omega_0\varsigma^T(t)A^TP\varsigma(t) + 2\varsigma^T(t)PB\times\frac{h(x(t),u(t),d(t),\dot{d}(t)) - h(\hat{x}(t),u(t),d(t),\dot{d}(t))}{\omega_0^n} = \\
&-\omega_0\left\|\varsigma(t)\right\|^2 + 2\varsigma^T(t)PB\times(h(x(t),u(t),d(t),\dot{d}(t)) - h(\hat{x}(t),u(t),d(t),\dot{d}(t)))/\omega_0^n.
\end{aligned} \tag{51}$$

According to assumptions (2) and (3) there exists a constant c'in such a way that $\left|h(x(t),u(t),d(t),\dot{d}(t)) - h(\hat{x}(t),u(t),d(t),\dot{d}(t))\right| \leq c'\left\|x(t) - \hat{x}(t)\right\|$ and so for (51)

$$\begin{aligned}
&2\varsigma^T(t)PB\tfrac{h(x(t),u(t),d(t),\dot{d}(t)) - h(\hat{x}(t),u(t),d(t),\dot{d}(t))}{{\omega_0}^n} \\
&\leq 2\varsigma^T(t)PB\tfrac{\left|h(x(t),u(t),d(t),\dot{d}(t)) - h(\hat{x}(t),u(t),d(t),\dot{d}(t))\right|}{{\omega_0}^n} \\
&\leq 2\varsigma^T(t)PB\tfrac{c'\left\|x(t)-\hat{x}(t)\right\|}{{\omega_0}^n},
\end{aligned} \tag{52}$$

where $\omega_0 \geq 1$and we can say that $\frac{\left\|x(t)-\hat{x}(t)\right\|}{{\omega_0}^n} = \frac{\left\|\tilde{x}(t)\right\|}{{\omega_0}^n} = \frac{\left\|\sqrt{{\varsigma_1}^2(t) + {\varsigma_2}^2(t)\omega_0^2 + \ldots + {\varsigma_{n+1}}^2(t)\omega_0^{2n}}\right\|}{{\omega_0}^n} \leq \left\|\varsigma(t)\right\|$. Therefore

$$\begin{aligned}
&2\varsigma^T(t)PB\times \\
&\tfrac{h(x(t),u(t),d(t),\dot{d}(t)) - h(\hat{x}(t),u(t),d(t),\dot{d}(t))}{{\omega_0}^n} \leq \\
&2\varsigma^T(t)PB\times \\
&\tfrac{\left|h(x(t),u(t),d(t),\dot{d}(t)) - h(\hat{x}(t),u(t),d(t),\dot{d}(t))\right|}{{\omega_0}^n} \leq \\
&2\varsigma^T(t)PB\tfrac{c'\left\|x(t)-\hat{x}(t)\right\|}{{\omega_0}^n} \leq 2\varsigma^T(t)PBc'\left\|\varsigma(t)\right\| \\
&\leq \left\|\varsigma(t)\right\|^2 + \left\|PBc'\right\|^2\left\|\varsigma(t)\right\|^2 = c\left\|\varsigma(t)\right\|^2,
\end{aligned} \tag{53}$$

where $c = 1 + \left\|PBc'\right\|^2$. So

$$\dot{Z}(t) \leq -(\omega_0 - c)\left\|\varsigma(t)\right\|^2. \tag{54}$$

This means that $\dot{Z}(t) < 0$ if $\omega_0 > c$. Also, by inserting (36) and (51) in (49), after mathematical simplification, $\dot{V}(t)$ can be written as below.

$$\begin{aligned}
&\dot{V}(t) \leq -\tfrac{1}{2}\hat{s}^T(t)\hat{s}(t) - \tfrac{1}{2}\lambda\left\|\tilde{x}(t)\right\|^2 - (\omega_0 - c)\left\|\varsigma(t)\right\|^2 \\
&-l_H\Phi_H(t)\theta_H(t) - \alpha(t)\left\|R\hat{s}(t)\right\|^2 u_0(t) + \left\|R\hat{s}(t)\right\|\Upsilon + \chi,
\end{aligned} \tag{55}$$

where $\chi = \chi_F + \chi_1$. The following relationship always holds:

$$\Phi\theta = \Phi(\Phi + \theta^*) \geq \frac{1}{2}\Phi^2 - \frac{1}{2}\theta^{*2}. \tag{56}$$

By using Young's inequality $2a^T b \leq \|a\|^2 + \|b\|^2$ and (36) and (37):

$$\begin{array}{l} \|R\hat{s}(t)\|\,\Upsilon - \alpha(t)\,\|R\hat{s}(t)\|^2 u_0(t) \leq \lambda_0 \|R\hat{s}(t)\|^2 \Upsilon^2 + \frac{1}{4\lambda_0} \\ +\lambda_0\alpha(t)N(\zeta)\,\|R\hat{s}(t)\|^2 \Upsilon^2 = (1+\alpha(t)N(\zeta))\dot{\zeta}(t) + \frac{1}{4\lambda_0}. \end{array} \tag{57}$$

Substituting (56) and (57) in (55), yields:

$$\begin{array}{l} \dot{V}(t) \leq -\frac{1}{2}\hat{s}^T(t)\hat{s}(t) - \frac{1}{2}\lambda\,\|\tilde{x}(t)\|^2 - \\ \frac{1}{2}l_H{\Phi_H}^2(t) - (\omega_0 - c)\,\|\varsigma(t)\|^2 + (1+\alpha(t)N(\zeta))\dot{\zeta}(t) \\ +\beta \leq -\alpha V(t) + \beta + (1+\alpha(t)N(\zeta))\dot{\zeta}(t) - (\omega_0 - c)\,\|\varsigma(t)\|^2, \end{array} \tag{58}$$

where

$$\alpha = \min\{1, \lambda/\lambda_{\max(p)}, \eta_F l_F\},$$

$$\beta = \frac{1}{2}l_F(\theta_F^*(t))^2 + \frac{1}{4\lambda_0} + \chi.$$

By multiplying both sides in $e^{\alpha t}$, (55) can be rewritten as follows.

$$\frac{d}{dt}(Ve^{\alpha t}) \leq \beta e^{\alpha t} + e^{\alpha t}(1+\alpha(t)N(\zeta))\dot{\zeta} - e^{\alpha t}(\omega_0 - c)\,\|\varsigma\|^2. \tag{59}$$

Integrating from (56) in the interval $[0, t]$, we will have:

$$V(t) \leq \frac{\beta}{\alpha} + V(0) + e^{-\alpha t}\int_0^t (1+\alpha(\tau)N(\zeta))\dot{\zeta}(\tau)e^{\alpha\tau}d\tau - \frac{1}{\alpha}(\omega_0 - c)e^{-\alpha t}\int_0^t \|\varsigma(\tau)\|^2 e^{\alpha\tau}d\tau. \tag{60}$$

Since $Z(t)$ is a decreasing function (because the result of (54) showed that $\dot{Z}(t) < 0$), then it converges to a finite value. Therefore, it can be said that the vector $\varsigma(t)$ is limited and bounded, as a result, it can be said that it will be $\varsigma(t) \in L_\infty$, therefore we can conclude that

$$\begin{array}{l} e^{-\alpha t}\int_0^t \|\varsigma(\tau)\|^2 e^{\alpha\tau}d\tau \leq e^{-\alpha t}\int_0^t {\|\varsigma\|_\infty}^2 e^{\alpha\tau}d\tau \leq \\ e^{-\alpha t}{\|\varsigma\|_\infty}^2 \int_0^t e^{\alpha\tau}d\tau \leq \frac{1}{\alpha}{\|\varsigma\|_\infty}^2(1 - e^{-\alpha t}) \leq \frac{1}{\alpha}{\|\varsigma\|_\infty}^2, \end{array} \tag{61}$$

and so, for (60)

$$\begin{array}{l} V(t) \leq \frac{\beta}{\alpha} + V(0) + e^{-\alpha t}\int_0^t (1+\alpha(\tau)N(\zeta))\dot{\zeta}(\tau)e^{\alpha\tau}d\tau \\ -\frac{1}{\alpha}(\omega_0 - c)e^{-\alpha t}\int_0^t \|\varsigma(\tau)\|^2 e^{\alpha\tau}d\tau \leq \\ \frac{\beta}{\alpha} + V(0) - \frac{1}{\alpha^2}(\omega_0 - c)\,{\|\varsigma\|_\infty}^2 + \\ e^{-\alpha t}\int_0^t (1+\alpha(\tau)N(\zeta))\dot{\zeta}(\tau)e^{\alpha\tau}d\tau. \end{array} \tag{62}$$

Term $\frac{\beta}{\alpha} + V(0) - \frac{1}{\alpha^2}(\omega_0 - c)\,{\|\varsigma\|_\infty}^2 = c_0$ is constant and bounded. According to lemma 2 [24],$V(t)$, $\int_0^t (1 + \alpha(\tau)N(\zeta))\dot{\zeta}(\tau)d\tau$ and $\zeta(t)$ are semi-globally uniformly ultimately bounded in the $[0, t_f)$. Therefore, $\hat{s}(t)$, $\|\tilde{x}(t)\|$, $\theta_H(t)$are semi-globally uniformly ultimately bounded (SUUB) in the $[0, t_f)$. From (29), $\hat{\varepsilon}(t)$ is bounded [25]. According to [4], $\hat{e}(t)$and its derivatives are bounded up to $r-1$, R *and* v are also bounded in the interval $[0, t_f)$. We can easily conclude that u is bounded by (33) and (36). Similar to [20], the above conclusion is also true $t_f = +\infty$. Therefore, all the signals are semi–globally uniformly ultimately bounded. Also, according to (54) that ensures$\dot{Z} < 0$, we can say that $\lim_{t\to\infty}\varsigma(t) \to 0$, and as a result, it is concluded that the estimation error of the extended state observer in the ADRC controller asymptotically converges to zero. □

4 Simulation results

In this part, the performance of the proposed hierarchical ACC system is evaluated through three scenarios. The results are compared to a predictive controller designed in the reference [28]. Fuzzy Adaptive Controller (FAC) typically involves simpler computations based on fuzzy logic rules and membership functions. The computational cost primarily comes from evaluating fuzzy rules and defuzzification processes, which are generally less intensive than optimization calculations. FAC can operate in real-time with relatively low delays, making it suitable for applications requiring quick responses. FACs Well-suited for systems with uncertainties and nonlinearities where a precise model is hard to obtain. Compared to that Model Predictive Control (MPC) involves solving an optimization problem at each control step, which may require significant computational resources, especially for complex systems with multiple states and constraints. The computational load increases with the prediction horizon and the number of constraints, making real-time implementation more challenging.

4.1 First scenario:

At the beginning of this scenario, they are stationary at a certain distance from each other. First, the car in front starts to accelerate in the time interval of zero to 20 seconds and brakes in the time interval of 25 to 40 seconds, and starts to accelerate again after that.

Description of the first scenario: The results in Fig. 4 show that the fuzzy controller has tracked the reference signal with much higher accuracy than the predictive controller. The acceleration signal has fewer fluctuations, which makes the passengers more comfortable. Also, the percentage of throttle opening angle in the fuzzy controller is lower, which leads to more economical fuel consumption, and as a result, less environmental pollution. The numerical improvement of the obtained results is given in Table. 3.

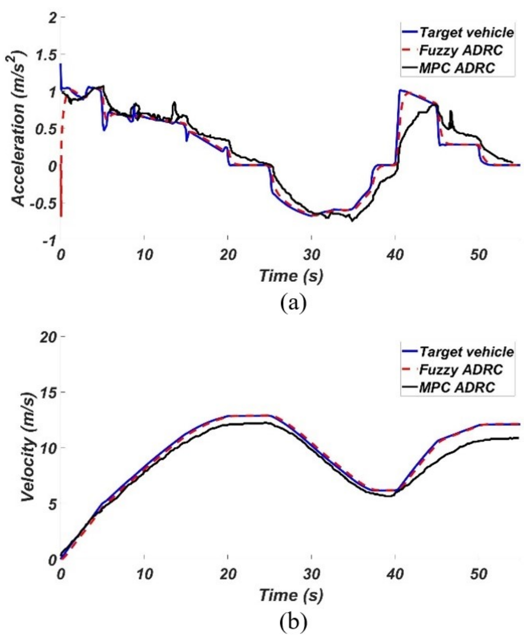

Figure 4: comparison results for Adaptive Fuzzy ADRC and MPC ADRC Controllers in the first scenario. (a). acceleration (b). velocity

Table 3 Improving the results of the fuzzy controller compared to the predictive controller in the first scenario with IAE

Improved opening throttle angle(decrease)	Improved velocity tracking	Improved acceleration tracking
%51.96	%37.94	%21.25

4.2 Second scenario:

In this scenario, internal and external disturbances have been applied to the car. The mass of the car has been increased by 200 Kg and it has changed to an uphill slope with a slope of 5 degrees. The results are as follows.
Description of the second scenario: From a and b in Fig. 5, the tracking of the host car is much more accurate than the front car. It can also be seen that the fuzzy adaptive controller can effectively neutralize the effect of internal and external disturbances (which here means the overload on the car and the road slope) and have accurate tracking of the front car. The statistics in Table. 4 show the improvement of the fuzzy adaptive controller compared to the predictive controller. In this scenario, the amount of throttle opening angle for the fuzzy adaptive controller was much less than the predictive controller, which caused a reduction in vehicle fuel consumption and increased efficiency of this adaptive cruise system. In addition, due to the more accurate tracking and guarantee of stability for this system, two cars will not collide under any circumstances. Also, the fluctuations and changes in the acceleration of the car are less in this mode, which will make the passengers more comfortable.

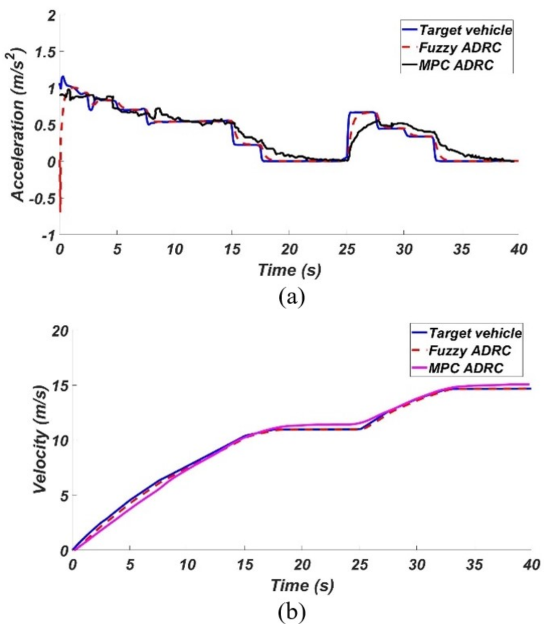

Figure 5: comparison results for Adaptive Fuzzy ADRC and MPC ADRC Controllers second scenario. (a). acceleration (b). velocity

Table 4 Improving the results of the fuzzy controller compared to the predictive controller in the second scenario with IAE

Improved opening throttle angle(decrease)	Improved velocity tracking	Improved acceleration tracking
%59.42	%51.59	%26.07

4.3 Third scenario

In this scenario, internal and external disturbances have changed. The mass added to the car is 200 Kg, with the difference that the slope of the road is 5 degrees, but it will be downhill. In this case, due to the downhill, the car will accelerate faster. The simulation results are as follows.
Description of the third scenario**:** Since in this case the following two cars are downhill from each other; therefore, the opening of the throttle angle decreases and instead the pressure on the brake pedal increases. As it is clear from a and b in Fig. 6, the following of the car by the fuzzy adaptive controller is much more accurate, the equivalent value of opening the throttle angle and pressure on the brake pedal is much lower than the case of using a predictive controller. This leads to a reduction in fuel consumption and air pollution, while the car accelerates and soft braking, which has the comfort of passengers, is provided. Also, the act of removing external disturbances applied to the car, which is the slope of the road, is well compensated by the active disturbance rejection controller and could not cause two cars to

collide with each other or reduce the efficiency of the designed cruise control system. The numerical improvement of the obtained results is given in Table. 5.

The computational intensity of a fuzzy adaptive controller in an autonomous vehicle is significant due to the complexity of real-time decision-making processes and the need to handle numerous inputs and outputs. The effective factors in computational intensity can be divided as follows:

-Number of Fuzzy Rules: The more fuzzy rules in the system, the more processing power is required. Each rule needs to be evaluated based on the current input state.

-Number of Inputs and Outputs: More inputs and outputs increase the complexity of the fuzzy inference process. Each input variable can have multiple membership functions, and the outputs need to be computed based on the combination of these inputs.

-Membership Functions: The type and number of membership functions affect computational load. Gaussian membership functions, for example, are computationally more intensive than triangular or trapezoidal functions.

-Real-time Constraints: Autonomous vehicles operate in real-time, requiring the controller to process data and make decisions within milliseconds. This necessitates highly efficient computation.

-Adaptive Mechanism: The adaptive component adds another layer of complexity, as it involves continuous learning and adjustment of the fuzzy rules based on feedback from the environment.

To meet these computational demands, a typical hardware setup for deploying a fuzzy adaptive controller in an autonomous vehicle might include:

CPU: Intel Core i9 or AMD Ryzen 9 with multiple cores and high clock speed.

GPU: NVIDIA RTX series GPU for parallel processing capabilities.

FPGA: Xilinx or Altera FPGA for implementing specific fuzzy logic operations.

RTOS: A real-time operating system like QNX or VxWorks.

Memory: At least 16 GB of DDR4/DDR5 RAM.

Sensors: High-resolution LiDAR, and radar integrated with a real-time data acquisition system.

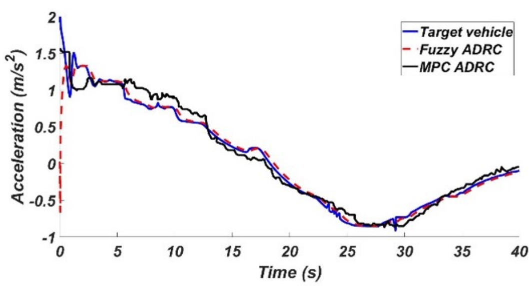

(a)

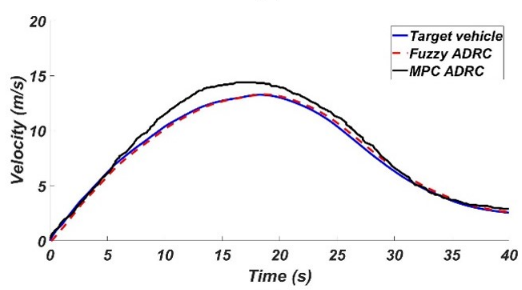

(b)

Figure 6: comparison results for Adaptive Fuzzy ADRC and MPC ADRC Controllers in the third scenario. (a). acceleration (b). velocity

Table 5 Improving the results of the fuzzy controller compared to the predictive controller in the third scenario with IAE

Improved opening throttle angle(decrease)	Improved velocity tracking	Improved acceleration tracking
%51.16	%46.28	%22.44

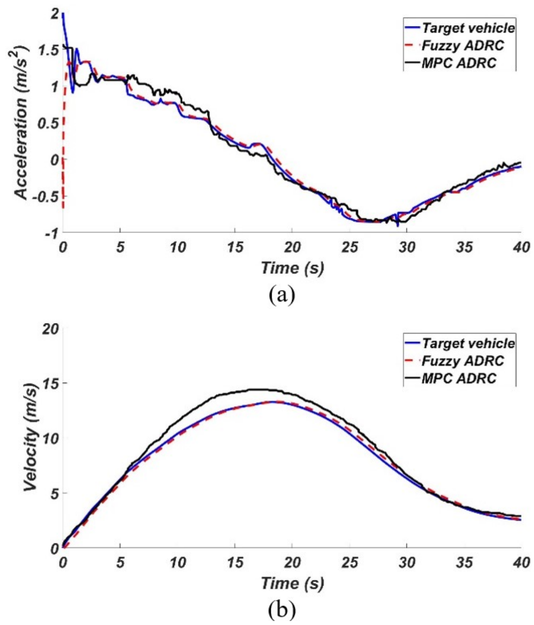

Figure 7: comparison results for Adaptive Fuzzy ADRC and MPC ADRC Controllers in the third scenario. (a). acceleration (b). velocity

Table 5 Improving the results of the fuzzy controller compared to the predictive controller in the third scenario with IAE

Improved opening throttle angle(decrease)	Improved velocity tracking	Improved acceleration tracking
%51.16	%46.28	%22.44

5 Conclusion

In this paper, a hierarchical ACC structure is proposed to control the longitudinal movement of a vehicle. The controller has two levels. A fuzzy adaptive output feedback controller with a certain efficiency criterion was designed and implemented as the upper-level controller. Also, an active disturbance rejection controller as the lower-level controller was used to eliminate the effect of internal and external disturbances. The ADRC parameters are tuned via a metaheuristic optimization. The stability of the proposed scheme is investigated and ensured. The proposed structure is

robust against large disturbances like as sudden changes in the speed of surrounding vehicles, abrupt braking by a lead vehicle, or unexpected lane changes. The system is designed to handle disturbances such that Speed changes of ± 15 km/h within 2 seconds, and Sudden deceleration of a lead vehicle (e.g., braking from 100 km/h to 50 km/h in less than 2 seconds), and wide uncertainties like as variability in vehicle mass, road friction coefficients, sensor noise, and environmental conditions. The system could account for uncertainties like Variations in vehicle mass of $\pm 10\%$ and Sensor measurement errors of $\pm 5\%$. To achieve the goals of improving passenger safety, accurate front car tracking, passenger comfort, reducing fuel consumption and emissions, as well as stability, a fuzzy adaptive controller is utilized. Eextensive simulations that model various driving scenarios, incorporating both large disturbances and wide uncertainties were conducted. These simulations allow for controlled testing of the ACC system's response to different conditions. The MPC strategy is a comparable approach that requires a model and has a significant computational load, unlike the proposed method. For comparison studies, three different scenarios are selected, and results are compared with an MPC controller. From the simulation results, it is shown that the designed controller meets all the desired criteria and the performance is significantly improved compared to a predictive controller.

References

[1] S. Akhegaonkar, L. Nouvelière, S. Glaser, F. Holzmann, *Smart and green ACC: Energy and safety optimization strategies for EVs*, IEEE Transactions on Systems, Man, and Cybernetics: Systems, **48**(1) (2018), 142-153. https://doi.org/10.1109/TSMC.2016.2600273

[2] A. S. Alghamdi, H. Eren, *Using fuzzy logic to control vehicles' velocity in traffic system*, IFAC Proceedings Volumes, **46**(10) (2013), 54-59.

[3] Z. Bareket, P. Fancher, H. Peng, K. Lee, C. Assaf, *Methodology for assessing adaptive cruise control behavior*, IEEE Transactions on Intelligent Transportation Systems, **4** (2003), 123-131. https://doi.org/10.1109/TITS.2003.821288

[4] C. P. Bechlioulis, G. A. Rovithakis, *Robust adaptive control of feedback linearizable MIMO nonlinear systems with prescribed performance*, IEEE Transactions on Automatic Control, **53**(9) (2008), 2090-2099. https://doi.org/10.1109/TAC.2008.929402

[5] N. Benalie, W. Pananurak, S. Thanok, M. Parnichkun, *Improvement of adaptive cruise control system based on speed characteristics and time headway*, in 2009 IEEE/RSJ International Conference on Intelligent Robots and Systems, 10-15 Oct. 2009, 2403-2408. https://doi.org/10.1109/IROS.2009.5353922

[6] Y. Bin, K. Li, X. Lian, H. Ukawa, M. Handa, H. Idonuma, *Longitudinal acceleration tracking control of vehicular stop-and-go cruise control system*, in IEEE International Conference on Networking, Sensing and Control, 2004, 21-23 March 2004 , 607-612. https://doi.org/10.1109/ICNSC.2004.1297508

[7] A. Boulkroune, M. M'Saad, M. Farza, *Adaptive fuzzy controller for multivariable nonlinear state time-varying delay systems subject to input nonlinearities*, Fuzzy Sets and Systems, **164**(1) (2011), 45-65. https://doi.org/10.1016/j.fss.2010.09.001

[8] T. Coen, J. Anthonis, J. De Baerdemaeker, *Cruise control using model predictive control with constraints*, Computers and Electronics in Agriculture, **63**(2) (2008), 227-236. https://doi.org/10.1016/j.compag.2008.03.003

[9] A. Ganguli, R. Rajamani, *Tractable model development and system identification for longitudinal vehicle dynamics*, Proceedings of the Institution of Mechanical Engineers, Part D: Journal of Automobile Engineering, **218**(10) (2004), 1077-1084. https://doi.org/10.1177/095440700421801002

[10] C. F. Hsu, W. J. Wang, T. T. Lee, C. M. Lin, *Longitudinal control of vehicle platoon via wavelet neural network*, in 2004 IEEE International Conference on Systems, Man and Cybernetics (IEEE Cat. No.04CH37583), 10-13 Oct. 2004 , 3811-3816. https://doi.org/10.1109/ICSMC.2004.1400938

[11] D. Kim, H. Peng, S. Bai, J. M. Maguire, *Control of integrated powertrain with electronic throttle and automatic transmission*, IEEE Transactions on Control Systems Technology, **15**(3) (2007), 474-482. https://doi.org/10.1109/TCST.2007.894641

[12] S. J. Ko, J. J. Lee, *Fuzzy logic based adaptive cruise control with guaranteed string stability*, in 2007 International Conference on Control, Automation and Systems, 17-20 Oct. 2007, 15-20. https://doi.org/10.1109/ICCAS.2007.4406871

[13] H. Lee, M. Tomizuka, *Adaptive vehicle traction force control for intelligent vehicle highway systems (IVHSs)*, IEEE Transactions on Industrial Electronics, **50**(1) (2003), 37-47. https://doi.org/10.1109/TIE.2002.807677

[14] L. Li, F. Y. Wang, Q. Zhou, *Integrated longitudinal and lateral tire/road friction modeling and monitoring for vehicle motion control*, IEEE Transactions on Intelligent Transportation Systems, **7**(1) (2006), 1-19. https://doi.org/10.1109/TITS.2005.858624

[15] C. Lu, A. Aakre, *A new adaptive cruise control strategy and its stabilization effect on traffic flow*, European Transport Research Review, **10**(2) (2018), 49. https://doi.org/10.1186/s12544-018-0321-9

[16] J. J. Martinez, C. Canudas-de-Wit, *A safe longitudinal control for adaptive cruise control and stop-and-go scenarios*, IEEE Transactions on Control Systems Technology, **15**(2) (2007), 246-258. https://doi.org/10.1109/TCST.2006.886432

[17] J. Na, Q. Chen, X. Ren, Y. Guo, *Adaptive prescribed performance motion control of servo mechanisms with friction compensation*, IEEE Transactions on Industrial Electronics, **61**(1) (2014), 486-494. https://doi.org/10.1109/TIE.2013.2240635

[18] J. E. Naranjo, C. Gonzalez, R. Garcia, T. D. Pedro, *ACC+Stop& go maneuvers with throttle and brake fuzzy control*, IEEE Transactions on Intelligent Transportation Systems, **7**(2) (2006), 213-225. https://doi.org/10.1109/TITS.2006.874723

[19] G. Naus, J. Ploeg, R. V. D. Molengraft, M. Steinbuch, *Explicit MPC design and performance-based tuning of an adaptive cruise control stop-&-go*, in 2008 IEEE Intelligent Vehicles Symposium, 4-6 June 2008, 434-439. https://doi.org/10.1109/IVS.2008.4621248

[20] R. D. Nussbaum, *Some remarks on a conjecture in parameter adaptive control*, Systems and Control Letters, **3**(5) (1983), 243-246. https://doi.org/10.1016/0167-6911(83)90021-X

[21] D. Ren, J. Zhang, *Adaptive algorithm to vehicle following control in intelligent transportation system*, in 2008 International Symposiums on Information Processing, 23-25 May 2008, 46-50. https://doi.org/10.1109/ISIP.2008.138

[22] P. Shakouri, A. Ordys, M. Askari, D. S. Laila, *Longitudinal vehicle dynamics using Simulink/Matlab*, in UKACC International Conference on Control 2010, 7-10 Sept. 2010, 1-6. https://doi.org/10.1049/ic.2010.0410

[23] L. Shengbo et al., *MPC based vehicular following control considering both fuel economy and tracking capability*, in 2008 IEEE Vehicle Power and Propulsion Conference, 3-5 Sept. 2008, 1-6. https://doi.org/10.1109/VPPC.2008.4677689

[24] W. Shi, *Adaptive fuzzy output-feedback control for nonaffine MIMO nonlinear systems with prescribed performance*, IEEE Transactions on Fuzzy Systems, **29**(5) (2021), 1107-1120. https://doi.org/10.1109/TFUZZ.2020.2969110

[25] J. J. E. Slotine, W. Li, *Applied nonlinear control*, Pearson, 1991.

[26] W. Wang, W. Zhang, H. Bubb, *Car-following safety algorithms based on adaptive cruise control strategies*, in 2007 5th International Symposium on Intelligent Systems and Informatics, 24-25 Aug. 2007, 135-140. https://doi.org/10.1109/SISY.2007.4342639

[27] Y. Xudong, J. Jingping, *Adaptive nonlinear design without a priori knowledge of control directions*, IEEE Transactions on Automatic Control, **43**(11) (1998), 1617-1621. https://doi.org/10.1109/9.728882

[28] Z. Yang, Z. Wang, M. Yan, *An optimization design of adaptive cruise control system based on MPC and ADRC*, Actuators, **10**(6) (2021), 110. https://doi.org/10.3390/act10060110

[29] Z. Zhang et al., *A vehicle active safety model: Vehicle speed control based on driver vigilance detection using wearable EEG and sparse representation*, (in eng), Sensors (Basel), **16**(2) (2016), 242.

[30] R. C. Zhao, P. K. Wong, Z. C. Xie, J. Zhao, *Real-time weighted multi-objective model predictive controller for adaptive cruise control systems*, International Journal of Automotive Technology, **18**(2) (2017), 279-292. https://doi.org/10.1007/s12239-017-0028-2